An analytical study on trotting at constant velocity and height*

Konstantinos Machairas, *Student Member, IEEE*, and Evangelos Papadopoulos, *Senior Member, IEEE*

Abstract—Quadrupedal trotting gaits of constant forward velocity and body height are studied. A method is developed, which is structured upon analytical expressions derived from the dynamics of a reduced single-legged model comprised of a point mass, and two actuated rotational joints. The inputs of the method include the robot mass, the leg and actuator properties, and the desired forward velocity, yielding all robot body feasible trajectories and their energy footprints. Thus, the method predicts the maximum forward velocity of a trotting quadruped; it also suggests energetically optimal combinations of body height and step length for a given forward velocity.

I. Introduction

Design and control are two key aspects in legged robotics. Interestingly, it is the coupling between them that raises the complexity in the attempt for bringing out optimized legged machines. An important class of open problems can be summarized as: given the design of a legged system and also a gait type, find the gait parameters that maximize or minimize a performance metric. Typical metrics include the maximum speed, the maximum payload etc.

To develop an optimized legged system, the locomotion task must be defined first. For example, a reasonable task is to move at the highest speed possible when carrying a certain payload. Second, the set of design and control parameters that satisfy the problem must be found. Typically, this process is very challenging for big generalized problems, due to the nonlinearity of the phenomena and the huge parameter space that must be searched. Analytical solutions are also rare to find. Therefore, making assumptions and studying simpler focused problems is a reasonable approach when searching for analytical expressions to gain insight into the problem and exploit them in design and control.

This work contributes with an analytical study on trotting at constant velocity and height. Based on the dynamics of a reduced single-legged model, answers are sought to the following questions. Given the robot design, the gait type, and the actuation system properties,

1. which body trajectories can achieve the desired velocity, and what are their energy footprints?
2. what is the maximum velocity that can be achieved?
3. which are the bottlenecks for the overall performance (e.g. low actuator torque capacity), and what are the possible improvements (e.g. adding reduction)?

To answer these, we focus on a specific gait that has been triggering the interest of biologists and engineers for more than 50 years, i.e. walking at constant forward velocity and body height. This gait was first studied back in 1953, and suggested that humans should keep the CoM trajectory close to a straight line to walk efficiently [1]. Along these lines, some of the first legged machines were built to move in this manner [2]. Although several researchers argued that the claims regarding energy efficiency were erroneous [3], such gaits are widely used; recently, Boston Dynamics quadrupeds performed impressive gaits of almost constant velocity and height in an unstructured environment [4].

From a control aspect, numerous works have proposed controllers that include toe trajectories with straight line parts [5], which also result in constant height locomotion. Since the dynamics are challenging to understand even for simple models, the gait has not received proper mathematical treatment so far. A major contribution of this work lies in deriving simple analytical expressions describing this gait.

Apart from the gait type, the leg design is specified in the beginning of this work. The two-segmented leg is chosen as a commonly used mechanism in quadruped robots. Two prevalent paradigms can be found for this type of leg, the serial two Degree of Freedom (DoF) leg [6], and the parallel two-DoF leg [7], [8]. This work focuses on the latter, aiming at the future application of the results on Laelaps II, a quadruped robot built at NTUA, whose legs are of this type [9].

II. The Method

The method examines legged robot trotting gaits of constant forward velocity and body height, see Fig 1. Its inputs include the robot mass, the leg and actuator properties, and the desired velocity, yielding all feasible trajectories of the body Center of Mass (CoM) and their energy footprints.
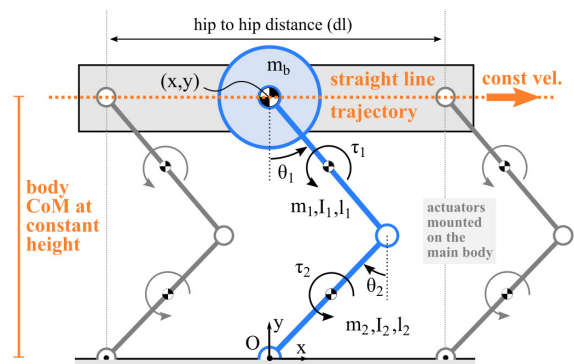

Figure 1. The initial 6-bar model comprised of two diagonal legs hinged to the ground (gray), and the reduced single-legged model (blue).

The study is structured upon the following steps:
 a. Selection of the desired locomotion task (gait),
 b. Selection of the leg design,
 c. Selection of a representative reduced dynamic model,
 d. Derivation of the equations of motion (EoM),
 e. Derivation of analytical expressions for the actuator requirements-discovery of feasible CoM trajectories,
 f. Trajectory characterization w.r.t. its energy footprint.

A. Locomotion task (gait)

A trotting quadruped moves two diagonal legs so that they contact the ground at the same time. Here, trotting of constant velocity and height is studied, focusing on the actuator requirements of the stance legs; power requirements for the swing legs are considered relatively low. Equal stance and swing phases are assumed, i.e., no aerial phases are included (always two legs contact the ground). Maintaining constant velocity means that the body does not accelerate and thus the ground forces are vertical (neglecting leg inertia). The gait resembles car-like or waiter-like motions and requires little friction, making it suitable for slippery terrains.

The aim behind this gait-specific study is twofold. First, numerous problems that legged robots may tackle require waiter-like gaits for example to affect their payload minimally. Second, with constant velocity and height, the analysis is simplified significantly, yielding minimal analytical expressions, which in turn can give insight and good estimations regarding numerous gaits of nearly constant (or slightly fluctuating) velocity and height.

B. Leg design

The study is also leg-specific, focusing on two-segmented legs with two actuators mounted on the main body. The hip actuator directly drives segment 1, while the knee actuator uses some transmission (e.g., parallel segments, cable/chain system etc.) to drive segment 2. Since both actuators are mounted on the body, the knee actuator controls the segment 2 angle w.r.t. the body, and not w.r.t. segment 1, which is the case in the serial two-segmented leg paradigm [6].

Two reasons lie behind this choice. First, the studied design is widespread in robotics [2], [7], [8], and yet not completely investigated; this study is useful in characterizing several existing robots, for example by giving a good estimation of their maximum trotting velocity, or by suggesting energetically optimal combinations of stride length and body height for a given velocity. Second, we aim at future validation of the results via direct application on Laelaps II [9], see Fig. 2, a quadruped robot featuring legs of this type. However, following the proposed steps also for other leg designs (e.g. a serial two-segmented leg [6]) will result in expressions that can be used in the same manner.

C. Selection of a representative reduced model

In case of a complex problem, using a reduced model facilitates the analytical approach at the expense of acquiring results of reduced – yet acceptable – precision. A good model for this study can be considered a 2D projection of a 3D

trotting model, yielding a planar 6-bar mechanism; two diagonal legs contact the ground with contacts modeled as pin joints (Fig. 1). However, the two actuators per leg make the mechanism over-actuated and hard to study. Therefore, aiming at intuitive analytical expressions, a further reduction is attempted, assuming that a planar two-segmented monopod with two virtual actuators of double torque capacity driving two virtual segments of double inertia and mass describes the task reasonably well. Since a fore and a hind leg always perform the same motion, the body pitching angle is assumed to be invariant, and the body is modeled as a point mass (Fig. 1). A segment is modeled as a point mass at its middle and an inertia w.r.t. this point. This model is valid only if all legs have the same knee configuration. Also, since stability must be guaranteed always, the projection of the CoM to the ground must lie between the two leg footholds; otherwise, a gravity-driven destabilizing moment will make the robot fall.

D. Derivation of the EoM

The EoM are derived for the generalized coordinates $\mathbf{q} = [\theta_1, \theta_2]$, as described in Fig. 1 and (A1) in the Appendix.

$$\begin{aligned} \tau_1 &= H_{11}\ddot{\theta}_1 + H_{12}\ddot{\theta}_2 + h\dot{\theta}_2^2 + G_1 \\ \tau_2 &= H_{22}\ddot{\theta}_2 + H_{21}\ddot{\theta}_1 - h\dot{\theta}_1^2 + G_2 \end{aligned} \quad (1)$$

E. Actuator requirements

The CoM velocity is given w.r.t. the coordinate system (CS) O of Fig. 1 as a function of the joint angular rates by,

$$\begin{bmatrix} \dot{x} \\ \dot{y} \end{bmatrix} = \mathbf{J_v} \begin{bmatrix} \dot{\theta}_1 \\ \dot{\theta}_2 \end{bmatrix}, \quad \mathbf{J_v} = \begin{bmatrix} -l_1 c_1 & -l_2 c_2 \\ -l_1 s_1 & -l_2 s_2 \end{bmatrix} \quad (2)$$

where $s_i = \sin\theta_i$, $c_i = \cos\theta_i$, $s_{i-j} = \sin(\theta_i - \theta_j)$, etc.

The joint angular rates are given as functions of the CoM velocity (except for the cases of singular configurations i.e., $\theta_1 - \theta_2 = n\pi$, $n = 0, \pm 1, \dots$) by,

$$\begin{bmatrix} \dot{\theta}_1 \\ \dot{\theta}_2 \end{bmatrix} = \mathbf{J_v^{-1}} \begin{bmatrix} \dot{x} \\ \dot{y} \end{bmatrix}, \quad \mathbf{J_v^{-1}} = \begin{bmatrix} s_2 / (l_1 s_{1-2}) & -c_2 / (l_1 s_{1-2}) \\ -s_1 / (l_2 s_{1-2}) & c_2 / (l_2 s_{1-2}) \end{bmatrix} \quad (3)$$

For $\dot{y} = \ddot{y} = \ddot{x} = 0$ (constant body CoM height and constant forward velocity) the joint angular rates become,

$$\dot{\theta}_1 = \frac{s_2}{l_1 s_{1-2}}\dot{x}, \quad \dot{\theta}_2 = \frac{-s_1}{l_2 s_{1-2}}\dot{x} \quad (4)$$

Differentiating (4) and using it again to eliminate $\dot{\theta}_1, \dot{\theta}_2$ yields,

$$\ddot{\theta}_1 = \frac{(s_1\dot{\theta}_2 - c_{1-2}s_2\dot{\theta}_1)}{l_1 s_{1-2}^2}\dot{x} \overset{(4)}{=} -\frac{(l_1 s_1^2 + l_2 c_{1-2}s_2^2)}{l_1^2 l_2 s_{1-2}^3}\dot{x}^2 \quad (5)$$

$$\ddot{\theta}_2 = \frac{(s_2\dot{\theta}_1 - c_{1-2}s_1\dot{\theta}_2)}{l_2 s_{1-2}^2}\dot{x} \overset{(4)}{=} \frac{(l_2 s_2^2 + l_1 c_{1-2}s_1^2)}{l_1 l_2^2 s_{1-2}^3}\dot{x}^2 \quad (6)$$

Replacing (5), (6) in the EoM, the stance torques are given by,

$$\tau_1 = \frac{(l_1^2 m_1 - 4I_1)(l_1 s_1^2 + l_2 s_2^2 c_{1-2})}{4 l_1^2 l_2 s_{1-2}^3}\dot{x}^2 - \frac{(m_1 + 2m_b)g l_1 s_1}{2} \quad (7)$$

$$\tau_2 = \frac{(l_2^2(2m_1 + m_2) + 4I_2)(l_2 s_2^2 + l_1 s_1^2 c_{1-2})}{4 l_1 l_2^2 s_{1-2}^3}\dot{x}^2 - (m_1 + \frac{m_2}{2} + m_b)g l_2 s_2 \quad (8)$$

Observation 1: With all the CoM positions w.r.t. the CS O (Fig. 1) lying on an annulus, (4) indicates that for every CoM position, the required hip and knee angular rates increase linearly with the forward velocity. Thus, knowing the actuator peak angular rates, one knows which CoM positions are reachable for a given forward velocity.

Observation 2: Given the forward velocity, and using (7) and (8), one can find the required joint torques for all body CoM positions; the required torques for some forward velocity are only configuration dependent. In this way, knowing the actuator torque capabilities, one can know which body positions are reachable for a given velocity.

Observation 3: Two terms appear in (7) and (8): one independent of the forward velocity – responsible for lifting the body weight and dependent only on the current configuration – and a second one dependent both on the current configuration and also on the square of the velocity.

Observation 4: The structure of (7) and (8) indicates that for each body CoM position, higher forward velocities require higher actuator torques. This means that for the same step length and body height combination, for higher velocity, higher hip and knee torques will be required.

F. Energy footprint of a trajectory

The power of an actuator with and without regeneration capabilities is given by (9) and (10) respectively, where K_t is the motor torque constant, R the motor terminal resistance, r the reduction ratio and $i = 1, 2$ a hip/knee index.

$$P_{reg,i} = P_{mech,i} + P_{el,i} = \tau_i \dot{\theta}_i + R_i \left(\frac{\tau_i}{r_i K_{t,i}} \right)^2 \quad (9)$$

$$P_{noreg,i} = \left| P_{mech,i} \right| + P_{el,i} = \left| \tau_i \dot{\theta}_i \right| + R_i \left(\frac{\tau_i}{r_i K_{t,i}} \right)^2 \quad (10)$$

The energy consumed by each actuator for a single step (using (9) or (10) depending on regeneration capabilities) is,

$$E_i = \int_0^T P_i \, dt \quad (11)$$

III. METHOD APPLICATION RESULTS

Here, the method is used to discover gaits for Laelaps II, a quadruped robot built by the Legged Team at the Control Systems Lab of NTUA [9], see Fig. 2. The robot parameters are given in Table I. The actuation system of each leg comprises two Maxon motors (RE50 for the hip, EC45 for the knee) combined with gearboxes and belt-pulley transmission systems. Since the knee motor is mounted on the body, a parallel mechanism is used to drive the distal leg segments. The two distal segments are considered equivalent to a single virtual rigid segment, since the connecting tendon-like spring is very stiff. The maximum torque/angular rate capabilities of the Laelaps II leg are 50Nm/55rpm for the hip, and 50Nm/75rpm for the knee; exceeding these limits will cause damage to the gearboxes, which are thus largely responsible for the drive-train limitations.
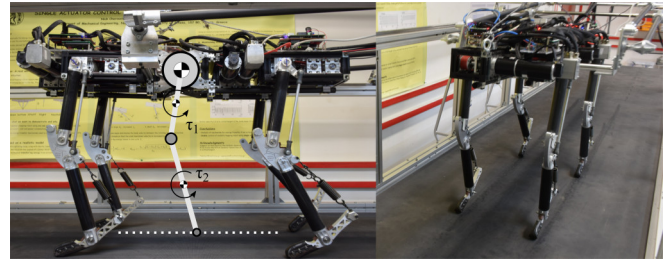

Figure 2. The quadruped robot Laelaps II, built by the Legged Team at the Control Systems Lab of NTUA [9], and the respective reduced single-legged model that was used in the analysis.

The derived expressions are evaluated for the robot properties given in Table I, the results are analyzed, and an attempt is made to reach generalized conclusions. Given a range of desired velocities, we find all the feasible body CoM trajectories for Laelaps II, and also the respective speed, torque and power requirements of the joints.

To this end, as the method requires, the whole system is reduced to a monopod hinged to the ground. The two legs contacting the ground are now represented by a virtual leg with double torque capabilities, double inertial properties, but same segment lengths and peak angular rates. Second, all the body CoM positions permitted by the kinematics (forming an annulus) are given w.r.t. the CS O of Fig. 1 as an input to the method, along with the desired forward velocity. Next, using the inverse kinematics for the specific configuration (knee-forward in this case, see Appendix), the corresponding hip-knee angle pairs are found. These together with the desired forward velocity are fed into (3) to find the required hip and knee angular rates, and in (7), (8) to find the required hip and knee torques for each body position. Finally, using (9) and (10) the power requirements are calculated for each position.

TABLE I.   LAELAPS II PARAMETERS.

Parameter	Value
Body mass m (kg)	40 kg
Hip to hip distance (dl)	0.6 m
Body inertia (I_b)	4 kgm^2
Segment 1 mass (m_1)	0.35 kg
Segment 2 mass (m_2)	0.8 kg
Segment 1 length (l_1)	0.25 m
Segment 2 length (l_2)	0.35 m
Max hip torque ($\tau_{1,max}$)	50 Nm
Max knee torque ($\tau_{2,max}$)	50 Nm
Max hip angular rate ($\dot{\theta}_{1,max}$)	55 rpm
Max knee angular rate ($\dot{\theta}_{2,max}$)	75 rpm
Hip motor rotor inertia (I_{r1})	0.0000542 kgm^2
Knee motor rotor inertia (I_{r2})	0.0000209 kgm^2
Hip motor torque constant ($K_{t,1}$)	93.4 mNm/A
Knee motor torque constant ($K_{t,2}$)	73.9 mNm/A
Hip motor terminal resistance (R_1)	0.608 Ω
Knee motor terminal resistance (R_2)	1.01 Ω
Hip actuator reduction ratio (r_1)	97.8462
Knee actuator reduction ratio (r_2)	79.3846
Seg. 1 inertia w.r.t. its CoM (I_1)	I_1 =0.5262 kgm^2
Seg. 2 inertia w.r.t. its CoM (I_2)	I_2 =0.1644 kgm^2

The method is first tested with zero forward velocity, corresponding to a static analysis of the system. Fig. 3 shows joint angular rate, torque and power requirements for all body reachable positions. The hip angular rates are shown in Fig. 3a and the hip torques in Fig. 3b. Similar plots are given in Fig. 3d and Fig. 3e for the knee joint. Interestingly, although the hip torque is adequate for keeping the body CoM in all positions, the knee actuator cannot support the body weight when the body CoM is placed in the white area of the annulus shown in Fig. 3e. The CoM positions that satisfy both angular rate and torque constraints are plotted in Fig. 3c for the hip actuator and in Fig. 3f for the knee actuator, and then colored based on their power requirements calculated using (9). Although angular rates are zero, power requirements are nonzero since the motors still draw current to produce the required torques; all the energy is converted to heat in the motor windings. Figs. 3c and 3f show the hip and knee power requirements separately; however only the intersection of the two sets of positions is the final set of reachable positions for the body CoM. Figs. 3h, 3i, 3j and 3k show this final set, colored based on the power requirements of each position, using (9), (10), with and without thermal losses. Plotting mechanical power gives insight into the mechanics of the task, and as expected, it is zero for the static case, Fig. 3j, 3k.

In the same manner, results are obtained for a desired forward velocity of 1.4 m/s, see Fig. 4. Comparing Figs. 4b, 4e, to Figs. 3b, 3e, a wide area in the annulus turns to white for 1.4 m/s, indicating that for those CoM positions the velocity dependent terms of (7), (8) increase and so do the torque requirements as the velocity increases. Regarding angular rates, results of which are shown in Figs. 4a and 4d, the structure of (4) is much simpler indicating that the hip and knee requirements in angular rate only increase as forward velocity increases for a specific CoM position. Figs. 4h, 4i, 4j, and 4k show that the positions the body can reach are significantly reduced, mainly due to the large demands in hip and knee torques; the hip and knee angular rates are lower than the actuator limits for most positions, Fig. 4a, 4d. Note also that the total mechanical power with regeneration, Fig. 4i is nonzero contrary to what would have been expected in the case of legs with zero inertial properties; in this case the hip and the knee power would cancel out to keep the body energy level constant as predicted by the gait studied herein.

Finally, the desired velocity is set to 2.4 m/s, Fig. 5. As expected due to (4), comparing Fig. 5a to Fig. 4a, the same positions inside the annulus now require higher angular rates, and as a result many positions that were reachable for 1.4 m/s, cannot be reached for 2.4 m/s. For this forward velocity, due to inadequate angular rate and torque capacity of the hip actuator and torque capacity of the knee actuator, there are almost no accessible body CoM positions, and the robot can only achieve this velocity with steps smaller than 10 cm, and with increased power requirements, see Figs. 5h, 5i, 5j, 5k.

Moreover, to avoid the details of Figs. 3-5 and to better identify the angular rate and torque limits of the system for a given velocity, a different graph can be used, as shown in Fig. 6. In these plots, using (4), (7) and (8) all body CoM positions that satisfy the inequalities related to the actuator limits $\dot{\theta}_1 < \dot{\theta}_{1,\max}$, $\dot{\theta}_2 < \dot{\theta}_{2,\max}$, $\tau_1 < \tau_{1,\max}$, $\tau_2 < \tau_{2,\max}$ are found for increasing values of the forward velocity $\dot{x}$. Thus, all reachable body CoM positions are shown for a wide range of forward velocities in a single graph.

The reader should read any subplot of Fig. 6 in the following way. First, choose a forward velocity by picking a color from the gray color bar, second, find the areas in the annulus filled with this color, then the reachable positions for the selected velocity are these that are filled with the selected color or any lighter shade of gray.

Figs. 6a-c correspond to limits set by the hip actuator, Figs. 6d-f correspond to the ones set by the knee actuator, and Figs. 6g-i give the total view of the robot limitations as the intersection of the hip and knee limitations. The maximum velocity of the robot can be achieved only in the area filled with the lighter shade of gray. Plotting all four constraints separately allows to find which subsystem of the actuation system is the real bottleneck.

In Fig. 6g, the blue trajectory is feasible for all velocities lower than 2 m/s. In Fig. 6h, the red trajectory cannot be followed by the robot CoM for any velocity for two different reasons; first, the trajectory starts from a horizontal position that lies behind the foothold of the hind leg which causes the robot to fall, and second, the end of the trajectory lies in the white area of the annulus meaning that these positions are forbidden even if the robot was standing still.

Design guidelines

As discussed above, the increased demands for torque at the knee and for angular rate and torque at the hip, hinder the robot from achieving velocities higher than 2.5 m/s. Regarding the knee actuator, which presents problems even for standing in several configurations (Fig. 3e), the high capacity in angular rate allows for increasing the reduction ratio to optimally exploit it. On the other hand, the hip actuator seems to be the real bottleneck for the system. Changes in the transmission ratio would probably have negative influence, since angular rate and torque constraints similarly affect the reachable CoM positions, Fig. 5a, 5b. To increase the maximum velocity, and without replacing the hip actuator, changes on the segment lengths should be considered. Methodologies for optimal selection of segment lengths have been proposed in [10].

Control guidelines

For each forward velocity, not every combination of stride length and body height are feasible. The controller must respect the limitations given by (4), (7) and (8) to avoid damaging the robot or forcing it to impossible tasks risking losing stability. An energy efficient controller would first find the reachable body CoM positions and then evaluate all feasible trajectories lying therein by finding the trajectories with the minimum energy footprint as calculated by (14). Also note that high stride frequencies improve gait stability but decrease efficiency due to energy loss through frequent collisions with the ground.
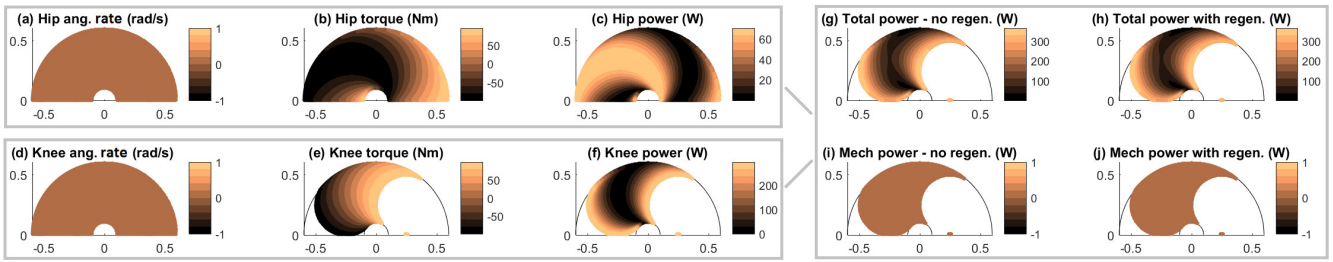
Figure 3. The annulus containing all possible body CoM positions is presented in colored plots to show the angular rate, torque and power requirements for each position. To obtain these plots, the method was fed with zero forward velocity, i.e. the robot is standing still in all possible positions. In Plots (a), (b) and (c) the areas filled with color concern the CoM positions for which the hip actuator does not exceed its torque/ang. rate limits. In Plots (d), (e), and (f) similar plots are presented for the knee actuator; the white areas in (e) show that the peak knee torque is not enough to lift the body weight in these positions. Plots (g), (h), (i), and (j) show the the CoM positions that both actuators can support, while the colors show the required power in each position; (g), and (h) show the total power (mechanical and Joule heating) without or with regeneration respectively, while (i) and (j) show only the total mechanical power.
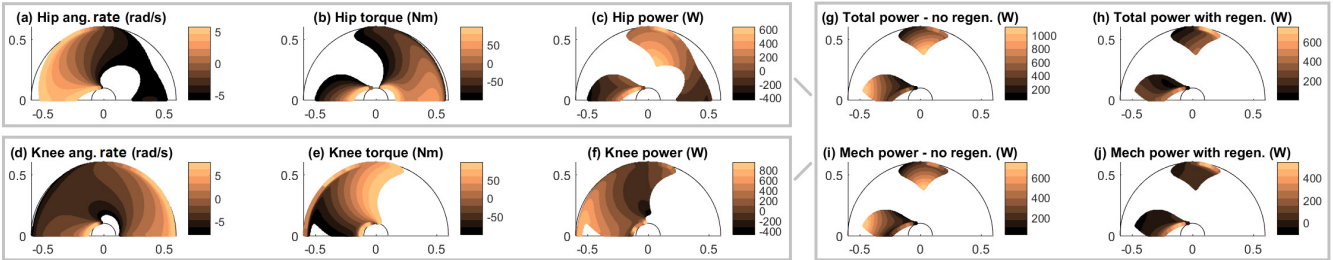

Figure 4. Results in the same format as described in Fig. 3 for a desired forward velocity of 1.4 m/s.
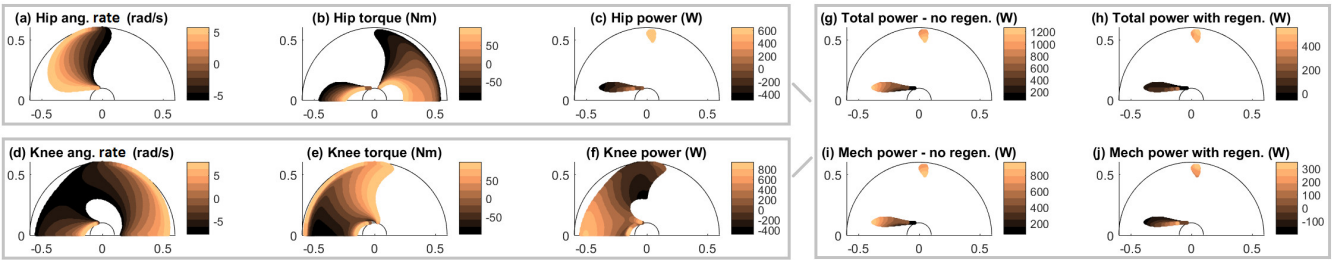

Figure 5. Results in the same format as described in Fig. 3 for a desired forward velocity of 2.4 m/s.
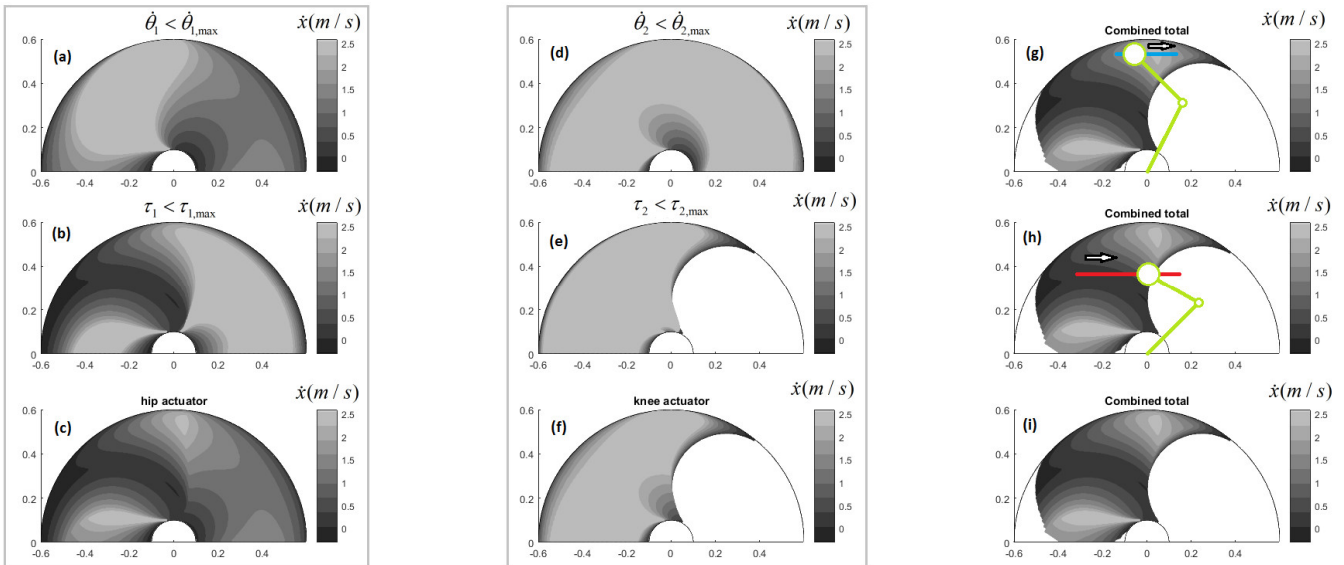

Figure 6. All body CoM positions that satisfy the inequalities related to the actuator limits are illustrated for increasing values of the forward velocity. Plots (a)-(c) correspond to limits set by the hip actuator, Plots (d)-(f) correspond to the ones set by the knee actuator, and Plots (g)-(i) give the total view of the robot limitations as the intersection of the hip and knee limitations. In Plot (g), the blue trajectory is possible for all forward velocities lower than 2 m/s. In Plot (h), the red trajectory cannot be followed by the robot CoM for any forward velocity.

IV. Discussion

The readers are encouraged to apply the method on other robots. From a design aspect, the analytical expressions given herein can be used to predict joint angular rates and torques depending on the forward velocity, to find the bottlenecks of an existing system, and to suggest changes regarding the actuators, the transmission ratios, the leg segment lengths etc. From a control aspect, the given expressions together with the resulting graphs can help to avoid damaging the actuation system by preventing it trying impossible trajectories. Moreover, using the method, efficient gaits can be found by properly choosing step length and body height combinations.

It is noted that, the expressions and results derived herein are task-dependent and are expected to change if other types of gaits are explored, e.g., SLIP-like gaits which predict body deceleration and acceleration for each stance phase. No body accelerations are considered here; only period-1 fixed points are searched for. Even if stable motions are discovered, there is no guarantee that the forward velocity found can be reached with the available torques. However, this is a secondary step, after finding the reachable fixed points and thus it is left as future work. Actuator requirements for accelerating the main body (changing its mechanical energy) is avoided due to the nature of the chosen gait. Although this is a major simplification, we show that significant bottlenecks appear at the acceleration of the leg segments; powerful motors are necessary even for such smooth gaits. In the scope of this work, the presented stable fixed points can be assumed to be reachable using very low body accelerations. Adding acceleration, will result in torque increments depending on the level of acceleration. For low accelerations, the results are expected to be close to those presented herein.

The virtual leg notion assumes that the two real legs are loaded equally during a step, however the leg closer to the body CoM bears a larger percentage of the body weight; this may result in asymmetrical torque requirements between the two legs and make the model reduction to a single virtual leg unsatisfactory. In that case, to validate predictions, simulation and experimentation is needed, especially for large steps.

The leg swing phase is considered less important in terms of joint angular rates and torques, and thus it was neglected. Yet, the required angular rates might rise in this phase, so further consideration is needed in a method revision.

Finally, peak continuous torques and RMS calculations were not included in this study and remain as future work. Here it was assumed that actuators will use the swing phase during the second-half of the stride period to cool down.

V. Conclusion

A method was presented for studying trotting gaits of constant forward velocity and body height. The method inputs include the leg properties, the actuation system properties, and the desired forward velocity, yielding all feasible trajectories of the robot CoM and the energy footprint for each trajectory. For the case of a two-DoF parallel leg design, analytical expressions were derived employing the dynamics of a reduced single-legged model. Based on these, the method predicts the maximum velocity of a given trotting quadruped and the actuator requirements for all lower velocities. Also, it suggests efficient combinations of body height and step length for a given desired velocity by calculating the power requirements for each trajectory.

References

[1] Saunders J. B. M., Inman, Verne T., and Howard D. Eberhart. "The major determinants in normal and pathological gait." *JBJS* 35.3, 1953: 543-558.

[2] Waldron, K. J., et al. "Mechanical and geometric design of the adaptive suspension vehicle." *Theory and Practice of Robots and Manipulators*. Springer, Boston, MA, 1985: 295-306.

[3] Kuo, A.D., "The six determinants of gait and the inverted pendulum analogy: A dynamic walking perspective." *Human Movement Science* v. 26. n. 4, 2007: 617-656.

[4] https://www.youtube.com/watch?v=Ve9kWX_KXus

[5] Barasuol, Victor, et al. "A reactive controller framework for quadrupedal locomotion on challenging terrain," *IEEE International Conference on Robotics and Automation (ICRA '13)*, Karlsruhe, Germany, 2013: 2554-2561.

[6] Hutter, Marco, et al. "Anymal-a highly mobile and dynamic quadrupedal robot." *IEEE/RSJ International Conference on Intelligent Robots & Systems* (*IROS '16*), Daejeon, Korea October 9-14, 2016.

[7] Asada, H., and K. Yousef-Toumi. *Direct Drive Robots: Theory and Practice*, MIT Press, Cambridge, MA, USA, 1987.

[8] Hubicki, Christian, et al. "ATRIAS: Design and validation of a tether-free 3D-capable spring-mass bipedal robot." *The Int. Journal of Robotics Research* 35.12 (2016): 1497-1521.

[9] http://nereus.mech.ntua.gr/legged/

[10] S. Dallas, K. Machairas, K. Koutsoukis and E. Papadopoulos, "A Leg Design Method for High Speed Quadrupedal Locomotion," *IEEE/RSJ Int. Conf. on Intelligent Robots and Systems (IROS)*, Vancouver, BC, Canada, 2017: 4877-4882.

APPENDIX A

EoM terms

$$H_{11} = I_1 + l_1^2(m_1/4 + m_b), \ H_{22} = I_2 + l_2^2(m_1 + m_2/4 + m_b),$$
$$H_{12} = H_{21} = l_1 l_2 c_{1-2}(m_1/2 + m_b), \ h = l_1 l_2 s_{1-2}(m_1/2 + m_b), \quad \text{(A1)}$$
$$G_1 = -l_1 g s_1(m_1/2 + m_b), \ G_2 = -l_2 g s_2(m_1 + m_2/2 + m_b)$$

Inverse kinematics

$$\theta_1 = \theta_2 + a\tan2(s,c)$$
$$\theta_2 = a\tan2(y,x) - a\tan2(l_1 s, l_2 + l_1 c) - \pi/2 \quad \text{(A2)}$$
$$c = (x^2 + y^2 - l_1^2 - l_2^2)/(2l_1 l_2), \ s = \pm\sqrt{1-c^2}$$